ELSEVIER

Coordination Chemistry Reviews 226 (2002) 103–111

COORDINATION CHEMISTRY REVIEWS

www.elsevier.com/locate/ccr

# Thermodynamic and structural aspects on the solvation steric effect of lanthanide(III)—dependence on the ionic size

S. Ishiguro *, Y. Umebayashi, M. Komiya

*Department of Chemistry, Faculty of Science, Kyushu University, Hakozaki, Higashi-ku, Fukuoka 812-8581, Japan*

Received 9 April 2001; accepted 15 October 2001

**Contents**



**Abstract**

Thermodynamic and structural aspects on the *solvation steric effect* for yttrium(III) and lanthanide(III) ions in DMF, DMA and their mixtures will be reviewed. The yttrium(III) and lanthanide(III) ions form outer- and inner-sphere bromo complexes in *N*,*N*-dimethylformamide (DMF) and *N*,*N*-dimethylacetamide (DMA), respectively, and an equilibrium geometry is established in the mixture. This is ascribed to the solvation steric effect of DMA, i.e. the simultaneous coordination of bulky DMA molecules around the metal ion causes a severe steric hindrance among them, allowing replacement of the solvent molecule with the penetrating bromide ion into the first-coordination sphere. Solvation steric effects for the metal(III) ion bring about appreciable changes in the bond length and solvation number. The results from titration calorimetry, EXAFS, $^{89}$Y-NMR and titration Raman spectroscopy will be discussed. 

*Keywords:* Lanthanide(III); Solvation steric effect; Complexation; DMF–DMA mixtures; Thermodynamics and structure

## 1. Introduction

We have so far studied metal-ion complexation in various aprotic donor solvents from the thermodynamic and structural point of view [1]. The solvation of metal ions plays a significant role in the metal-ion complexation in solution. Particularly, in bulky aprotic donor solvents such as *N*,*N*-dimethylacetamide (DMA), *N*,*N*-dimethylpropionamide (DMPA), *N*,*N*-dimethylbenzamide (DMBA), tetramethylurea (TMU), hexamethylphosphoric triamide (HMPA), etc. solvation steric effect operates among solvent molecules bound to the metal ion. A *strong solvation steric effect* brings about a reduced solvation number around the metal ion. Indeed, the nickel(II) ion is five-coordinate in DMPA and TMU (solution color is red), and four-coordinate in DMBA (blue). On the other hand, transition metal(II) ions show a *weak solvation steric effect* in DMA. A weak solvation steric effect leads to practically no change in the solvation number and bond length, while it leads to a significant distortion in the dihedral angle between solvent molecules. Both strong

* Corresponding author. Tel.: +81-92-642-2581; fax: +81-92-642-2607.

*E-mail address:* analsscc@mbox.nc.kyushu-u.ac.jp (S. Ishiguro).

0010-8545/02/$ - see front matter 
PII: S0010-8545(01)00448-9

and weak solvation steric effects result in a significantly enhanced complexation of the metal ion, mainly owing to an enthalpy term.

Much work has been devoted to the chemistry of lanthanide(III) ions [2], and in recent years, attention has been paid particularly to the macrocyclic complexes of lanthanide(III) [3]. The lanthanide(III) ion forms a variety of complexes in aprotic solvents [4,5]. Legendziewicz et al. have reported the solution structure of lanthanide(III) ions in nonaqueous solutions on the basis of luminescence spectra [6], where they conclude that the neodymium(III) ion is nine-coordinated in *n*-propanol and seven-coordinated in *i*-propanol owing to the steric effect. Recently, we found that bromo complexation shows significantly different thermodynamic behavior in DMF and DMA, i.e. the formation of enthalpy and entropy values are all small and positive without an appreciable metal-ion dependence in DMF, while the values are large and positive with a strong metal-ion dependence in DMA. The difference is explained in terms of formation of a solvent separated ion-pair or an outer-sphere complex in DMF, and the formation of a contact ion-pair or an inner-sphere complex in DMA [7]. As these solvents have similar molecular geometries and physicochemical properties such as relative dielectric constant, and electron-pair donating and accepting properties [8], the different complexation behavior in the solvents may be ascribed primarily to the *solvation steric effect*. As the DMA molecule involves the bulkier acetyl group, $-C(CH_3)O$, as compared with the formyl group, –CHO, of DMF, strong solvation steric hindrance operates when DMA molecules simultaneously coordinate to the lanthanide(III) ion with a larger coordination number than the transition metal(II) ions.

To obtain direct structural evidence on solvation steric effects, the solvation structure of lanthanide(III) ions in DMF, DMA and their mixtures has been studied by EXAFS (extended X-ray absorption fine structure) and $^{89}$Y-NMR [9–11]. The total solvation number of the metal ion can be determined by EXAFS as well as by X-ray diffraction. In a solvent mixture with similar coordinating abilities, the metal ion is solvated with both solvent components, and the individual solvation number plays an important role in the complexation behavior. However, the individual solvation number cannot be determined by EXAFS. We thus developed titration Raman spectrometry which was successfully applied to the solvation structure of the nickel(II) ion in DMF–DMA mixtures [12]. Here, we will review our recent work on the solvation steric effect of lanthanide(III) ions from thermodynamic and structural view-points.

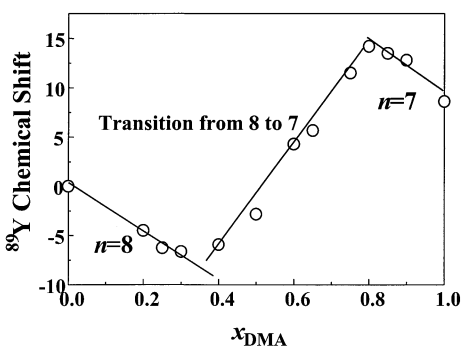


Fig. 1. Variation of $^{89}$Y-NMR chemical shift in the DMF–DMA mixtures plotted against the mole fraction $x$ of DMA.

## 2. Solvation structure

$^{89}$Y-NMR chemical shifts obtained in the DMF–DMA mixtures containing 0.1–0.2 mol dm$^{-3}$ $Y(ClO_4)_3$ are shown in Fig. 1. With increasing DMA content $x$ in the mixture, the $^{89}$Y-NMR signal shifts first to a higher magnetic field ($0 < x < 0.4$), then to a lower ($0.4 < x < 0.8$), and again to a higher ($0.8 < x < 1$). As the electron-pair donating ability of DMA is slightly stronger than that of DMF, the shift to a higher magnetic field can be explained in terms of a step-by-step replacement of bound DMF molecules with DMA without a coordination geometry change. On the other hand, the shift to a lower magnetic field indicates that the electron density around the yttrium(III) ion is reduced, i.e. the coordination number of the yttrium(III) ion is decreased. Indeed, the decreased coordination number has also been found by EXAFS for Tm(III) over almost the same range of solvent composition, as will be shown below. This is not unexpected because the ionic size of Y(III), which is similar to that of Ho(III) ($Z = 67$), is not significantly different from that of Tm(III) ($Z = 69$).

The structural parameters obtained by EXAFS for a series of $Ln(ClO_4)_3$ in water (ca. 0.8 mol dm$^{-3}$), DMF (ca. 0.8 mol dm$^{-3}$) and DMA (ca. 0.3 mol dm$^{-3}$) solutions are listed in Table 1. As the coordination numbers of 9 and 8 have been established for light and heavy lanthanide(III) ions in water, these values were fixed in the analyses. The Ln–O($H_2O$) bond lengths thus obtained agree satisfactorily with those by diffraction methods [13–16]. The Ln–O(DMF) and Ln–O(DMA) bond lengths can be determined with accuracy, while the coordination numbers, scattered in the range 6–9, are rather unreliable owing to difficulties in evaluating relatively large coordination numbers. Consequently, the variation of bond length gives more useful information for solvation structure of lanthanide(III) ions in solution. In Fig. 2, the Ln–O($H_2O$), Ln–O(DMF) and Ln–O(DMA) bond lengths are plotted against the atomic number $Z$. The bond length $r_{Ln-O}$ decreases monotonically with $Z$ for all the solvent

Table 1
Bond length, $r$ (pm), Debye–Waller factor, $\sigma$ (pm), and coordination number, $n$, for the Ln–O interaction of solvated ions in water, DMF and DMA

| Ions | Water | | | *N*,*N*-Dimethylformamide | | | *N*,*N*-Dimethylacetamide | | |
|---|---|---|---|---|---|---|---|---|---|
| | $r$ (pm) | $\sigma$ (pm) | $n$[a] | $r$ (pm) | $\sigma$ (pm) | $n$ | $r$ (pm) | $\sigma$ (pm) | $n$ |
| La(III) | 254.5 (0.2) | 8.5 (0.2) | 9 | 248.55 (0.07) | 8.6 (0.2) | 7.3 (0.2) | 247.45 (0.08) | 7.6 (0.2) | 6.5 (0.2) |
| Ce(III) | 253.8 (0.2) | 8.0 (0.2) | 9 | 247.4 (0.1) | 8.9 (0.2) | 8.1 (0.3) | 245.16 (0.05) | 9.0 (0.1) | 6.6 (0.1) |
| Pr(III) | 250.3 (0.2) | 8.8 (0.2) | 9 | 244.7 (0.1) | 8.6 (0.3) | 7.4 (0.3) | 241.97 (0.05) | 8.6 (0.1) | 6.9 (0.1) |
| Nd(III) | 248.8 (0.2) | 9.2 (0.2) | 9 | 243.82 (0.08) | 8.6 (0.2) | 7.4 (0.2) | 240.21 (0.08) | 7.7 (0.2) | 6.1 (0.2) |
| Sm(III) | 245.5 (0.1) | 8.1 (0.1) | 9 | 241.62 (0.04) | 8.40 (0.07) | 8.9 (0.1) | 236.69 (0.05) | 8.8 (0.1) | 8.4 (0.1) |
| Eu(III) | 242.4 (0.1) | 8.22 (0.09) | 8 | 238.53 (0.07) | 8.1 (0.1) | 7.7 (0.1) | 234.66 (0.04) | 7.70 (0.09) | 6.7 (0.09) |
| Gd(III) | 241.5 (0.2) | 7.8 (0.1) | 8 | 238.49 (0.06) | 7.5 (0.1) | 7.5 (0.1) | 233.27 (0.05) | 7.3 (0.1 | 7.2 (0.1) |
| Tb(III) | 239.0 (0.2) | 7.67 (0.08) | 8 | 236.85 (0.04) | 7.67 (0.07) | 7.54 (0.09) | 231.92 (0.05) | 7.75 (0.09) | 7.3 (0.1) |
| Dy(III) | 237.33 (0.08) | 7.57 (0.06) | 8 | 235.97 (0.07) | 8.0 (0.1) | 7.7 (0.2) | 230.48 (0.07) | 7.7 (0.1) | 7.0 (0.) |
| Ho(III) | 235.9 (0.1) | 7.43 (0.09) | 8 | 234.58 (0.07) | 8.0 (0.1) | 7.8 (0.2) | 229.26 (0.05) | 7.22 (0.08) | 6.88 (0.09) |
| Er(III) | 234.99 (0.07) | 7.61 (0.05) | 8 | 233.6 (0.04) | 7.58 (0.07) | 7.16 (0.08) | 227.32 (0.06) | 7.4 (0.1) | 7.6 (0.1) |
| Tm(III) | 233.4 (0.1) | 7.47 (0.07) | 8 | 232.4 (0.04) | 7.67 (0.07) | 7.5 (0.1) | 226.65 (0.04) | 7.32 (0.07) | 6.77 (0.08) |
| Yb(III) | 231.7 (0.1) | 7.27 (0.04) | 8 | 230.94 (0.04) | 7.70 (0.07) | 7.46 (0.09) | 223.83 (0.04) | 7.18 (0.06) | 6.33 (0.07) |
| Lu(III) | 230.98 (0.07) | 7.33 (0.05) | 8 | 229.75 (0.07) | 7.86 (0.06) | 7.87 (0.09) | 222.15 (0.04) | 7.08 (0.07) | 5.96 (0.07) |

Values in parentheses refer to a standard deviation.
[a] Fixed.

systems examined. The $r_{Ln-O}$ difference between Ln–O($H_2O$) and Ln–O(DMF) is significant for La(III), but it is not for Lu(III). This implies that the average coordination number in water is appreciably larger than that in DMF for La(III), while they are similar for Lu(III). As the lanthanum(III) ion is nine-coordinated to form $La(H_2O)_9^{3+}$ in water, the metal ion may be mainly eight-coordinate to form $La(DMF)_8^{3+}$ in DMF, while as the lutetium(III) ion is eight-coordinate to form $Lu(H_2O)_8^{3+}$ in water, the metal ion is also eight-coordinate to form $Lu(DMF)_8^{3+}$ in DMF [17,18]. We thus propose that the eight-coordinate $Ln(DMF)_8^{3+}$ ion is present as the main species in DMF throughout the lanthanide(III) series, although light lanthanide(III) ions (La(III)–Nd(III)) seems to be partly nine-coordinate according to our calorimetric study. Indeed, with $Ln(DMF)_n^{3+}$, the variation profile is similar to that of eight-coordinate compounds in the solid state [19]. A similar consideration is also applied to the coordination number in DMF and DMA. The $r_{Ln-O}$ of La–O(DMF) and La–O(DMA) are not appreciably different, suggesting that the La(III) ion has practically the same coordination number in both DMF and DMA. Interestingly, the $r_{Ln-O}$ difference becomes larger with $Z$, and the largest is seen in the Lu(III) ion, indicating that the coordination number is reduced to seven, or even less, in DMA, unlike DMF with eight-coordination. If these metal ions are assumed to be eight-coordinate in DMF and seven-coordinate in DMA, the coordination geometry changes from eight to seven with increasing DMA content in the DMF–DMA mixtures. Indeed, as mentioned above, the geometry transition has been pointed out for Tm(III) and Y(III) in the DMF–DMA mixtures. We thus propose that the La(III) ion exists mainly as the eight-coordinate $La(DMA)_8^{3+}$, while the Lu(III) ion exists mainly as the seven-coordinate $Lu(DMA)_7^{3+}$ in DMA. This is expected because DMA is bulkier than DMF, and a solvation steric hindrance is thus severe particularly for heavy lanthanide(III) ions with smaller ionic sizes. With light lanthanide(III) ions, the difference in $r_{Ln-O}$ is not so large as that for the Lu(III) ion, implying that a geometry equilibrium between eight- and seven-coordination is established in DMA.

## 3. Thermodynamics of complexation

Formation constants, enthalpies and entropies of bromo complexation of lanthanide(III) ions have simul-

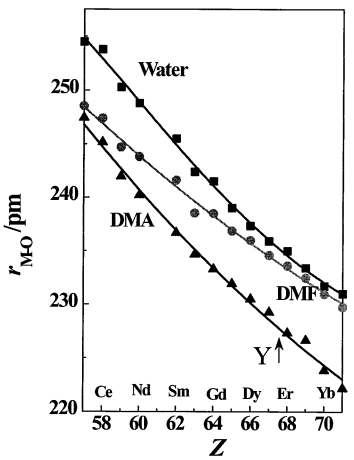


Fig. 2. Variation of the Ln–O bond length for lanthanide(III) in water, DMF and DMA.

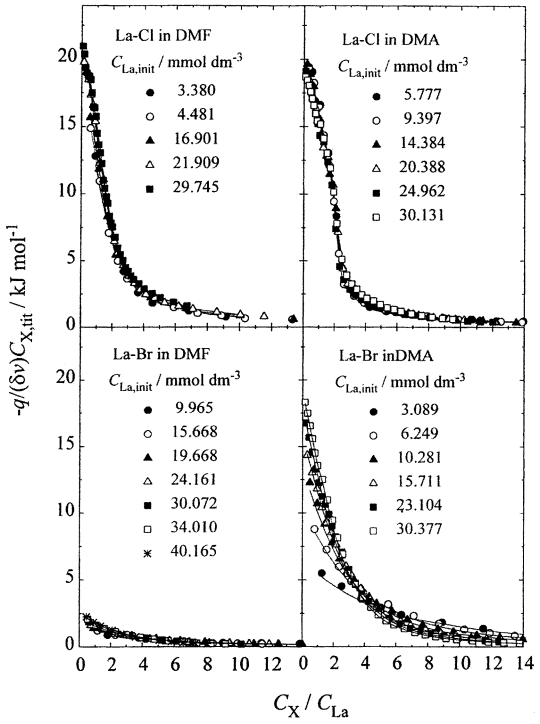


Fig. 3. Calorimetric titration curves in the La(III)–$Cl^-$ and La(III)–$Br^-$ systems in DMF and DMA at 298 K.

Table 2
Thermodynamic quantities, stepwise formation constant, log $K_n$ (mol $dm^{-3}$), enthalpies, $\Delta H_n^\circ$ (kJ $mol^{-1}$), and entropies, $\Delta S_n^\circ$ (J $K^{-1}$ $mol^{-1}$) of $LaX_n^{(3-n)+}$ (X = Cl, Br) in *N*,*N*-dimethylformamide and *N*,*N*-dimethylacetamide containing 0.2 mol $dm^{-3}$ $(C_4H_9)_4NClO_4$ as an ionic medium at 298 K

| | DMF | | DMA | |
|---|---|---|---|---|
| | Cl | Br | Cl | Br |
| Log $K_1$ | 3.04 (6) | 1.4 (2) | 4.1 (2) | 1.99 (5) |
| Log $K_2$ | 2.15 (8) | 0.4 (30) | 3.5 (2) | 1.56 (8) |
| Log $K_3$ | 0.4 (2) | – | 0.9 (2) | 1.0 (0.1) |
| $\Delta H_1^\circ$ | 21.2 (4) | 5 (1) | 19.1 (4) | 25 (1) |
| $\Delta H_2^\circ$ | 21 (1) | 25 (15) | 21.3 (3) | 20 (4) |
| $\Delta H_3^\circ$ | – | – | 34 (3) | 9 (5) |
| $\Delta S_1^\circ$ | 129 (1) | 42.9 (7) | 143 (1) | 122 (3) |
| $\Delta S_2^\circ$ | 82 (3) | – | 105 (5) | 96 (11) |
| $\Delta S_3^\circ$ | – | – | 130 (10) | 50 (15) |
| *N* | 96 | 67 | 118 | 124 |
| *R* | 0.0178 | 0.0336 | 0.0218 | 0.0188 |

Values in parentheses refer to three standard deviation at the last significant digits.

taneously been obtained by calorimetry. Typical calorimetric titration curves for the La(III)–$Br^-$ system in DMF and DMA, obtained by titrating a $La(ClO_4)_3$ solution with a $(C_4H_8)_4NBr$ solution containing 0.2 mol $dm^{-3}$ $(C_4H_8)_4NClO_4$ as an ionic medium at 298 K, are shown in Fig. 3, together with those for the La(III)–$Cl^-$ system. In the figure, the apparent enthalpy values $\Delta H^\circ = -q/(\delta v C_{X,tit})$ obtained at each titration point are plotted against the total concentration ratio of the halide to metal ions $C_X/C_{La}$ in solution, where $q$, $\delta v$ and $C_{X,tit}$ denote the measured heat of reaction, the volume of an aliquot of the added titrant and the concentration of the halide ion in the titrant solution, respectively. Calorimetric titration curves in DMF and DMA are similar for chloride, but significantly different for bromide. The titration curves can be explained satisfactorily in terms of the formation of mono- and di-bromo complexes in DMF, and the formation of mono-, di- and tri-bromo complexes in DMA, and the formation constants, enthalpies and entropies of formation of the complexes have been determined by nonlinear least-square analyses. The results are listed in Table 2. In both solvents, thermodynamic parameters for the mono–bromo complexation have been determined with accuracy with small Hamilton *R*-factors. Indeed, the solid lines in Fig. 3 show calculated curves on the basis of the formation constants and enthalpies finally obtained for the complexes, which reproduce well all experimental points.

Interestingly, calorimetric titration curves obtained for a series of lanthanides show a strong metal-ion dependence for the Ln(III)–$Br^-$ system in DMA, while this is not so for the Ln(III)–$Br^-$ system in DMF. This indicates that the bromide ion binds to the lanthanide(III) ions in DMA, while it does not in DMF to form solvent-separated ion-pairs in DMF. The enthalpy–entropy relationship for the mono–bromo complexes is shown in Fig. 4. Both enthalpy and entropy values for the bromo complexes in DMA are all positive and significantly larger than the corresponding values in DMF. The positive but relatively small $\Delta H_1^\circ$ and $\Delta S_1^\circ$ values in DMF also indicate the formation of ion-pairs or outer-sphere complexes, while the large $\Delta H_1^\circ$ and $\Delta S_1^\circ$ values in DMA clearly indicate the formation of inner-sphere complexes. Both $\Delta H_1^\circ$ and $\Delta S_1^\circ$ values show a big jump between Nd(III) and Sm(III) in DMA, suggesting that the coordination

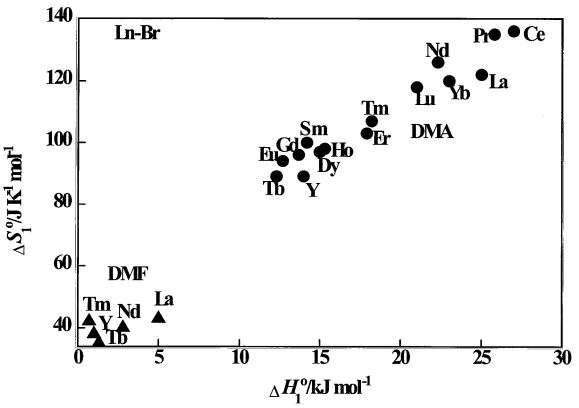


Fig. 4. The $\Delta S_1^\circ$ vs. $\Delta H_1^\circ$ plot for the Ln(III)–$Br^-$ system in DMF (▲) and DMA (●).

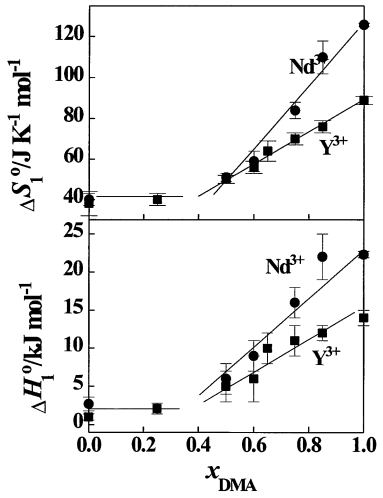


Fig. 5. Variation of $\Delta S_1^\circ$ and $\Delta H_1^\circ$ for the formation of $LnBr^{2+}$ (Ln = Nd, Y) in the DMF–DMA mixtures.

number of $[LnBr(DMA)_n]^{2+}$ changes at around those metal ions.

The formation enthalpies and entropies of the mono–bromo complexes of Nd(III) and Y(III) for the DMF–DMA mixtures are shown in Fig. 5. In neat DMF and in the mixture $x = 0.25$, the $\Delta S_1^\circ$ values are all close to 40, irrespective of the metal ion or the solvent composition, indicating the formation of an outer-sphere bromo complex. The entropy value is ascribed mainly to the desolvation of the bromide ion upon reaction, $Ln(solvent)_8^{3+} + Br^- = [Ln(solvent)_8^{3+}]\text{-}Br^-$. The $\Delta S_1^\circ$ value gradually increases with increasing DMA content at $x > 0.4$, and in the Y(III) system, the variation is completely in parallel with that for $^{89}$Y-NMR, as will be discussed below, indicating that the $\Delta S_1^\circ$ increase is coupled with the formation of an inner-sphere bromo complex. The $\Delta S_1^\circ$ increase is more marked for Nd(III) than Y(III). As the Nd(III) ion is eight-coordinate over almost the whole range of solvent composition in the DMF–DMA mixtures, the bromo complexation may proceed mainly via reaction, $Nd(solvent)_8^{3+} + Br^- = NdBr(solvent)_6^{2+} + 2$ solvent, i.e. two solvent molecules desolvate the metal ion. On the other hand, as the Y(III) ion is mainly seven-coordinate in the DMA-rich mixture, the possible complexation scheme may mainly be $Y(solvent)_7^{3+} + Br^- = YBr(solvent)_6^{2+} +$ solvent, i.e. one solvent molecule desolvates the metal ion. Therefore, it is proposed that the number of solvent molecules desolvating the metal ion upon complexation is larger for Nd(III) than Y(III). This must be the main reason for the entropy difference in the metal systems.

The $\Delta S_1^\circ$ values for a reaction, $Ln^{3+} + Br^- = LnBr^{2+}$, of a series of lanthanide(III) ions in DMA also lead to a similar conclusion. As the $\Delta S_1^\circ$ value in DMF is ca. 40 J K$^{-1}$ mol$^{-1}$ for all the lanthanide(III) ions, the difference entropy $\Delta\Delta S_1^\circ$ $\{= \Delta S_1^\circ$ (DMA) $- \Delta S_1^\circ$ (DMF)$\}$ is strongly related to the number of solvent molecule liberated upon complexation. The value is the largest (ca. 100 J K$^{-1}$ mol$^{-1}$) for Ce(III) and Pr(III). With increasing atomic number, the value gradually decreases with the least (ca. 50 J K$^{-1}$ mol$^{-1}$) for Tb(III), and then increases to ca. 80 J K$^{-1}$ mol$^{-1}$ for Yb(III) and Lu(III). This implies that two solvent molecules are liberated from the Ce(III) and Pr(III) ions upon complexation, while one solvent molecule is liberated from the Yb(III) ion, likeY(III). This is expected as the Ce(III) and Pr(III) ions are mainly eight-coordinate and the bromo complexation proceeds via reaction, $Ln(solvent)_8^{3+} + Br^- = LnBr(solvent)_6^{2+} +$ 2 solvent, in DMA, while the Yb(III) ion is mainly seven-coordinate and the complexation proceeds via reaction $Ln(solvent)_7^{3+} + Br^- = LnBr(solvent)_6^{2+} +$ solvent. The $\Delta\Delta S_1^\circ$ value decreases in the order Nd(III) > Sm(III) > Er(III) > Gd(III), suggesting that the equilibrium geometry is established between eight- and seven-coordination, and shifts towards seven-coordination in the same order. On the other hand, the $\Delta\Delta S_1^\circ$ value significantly increases in the order Dy(III) < Ho(III) < Er(III) < Tm(III) < Yb(III), all being seven-coordinate in DMA. These facts lead to the deduction that the six-coordinate $LnBr(solvent)_5^{2+}$ is formed according to $Ln(solvent)_7^{3+} + Br^- = LnBr(solvent)_5^{2+} +$ 2 solvent, together with the seven-coordinate $LnBr(solvent)_6^{2+}$. The six- and seven-coordinate mono–bromo complex may thus be simultaneously formed in equilibrium, and the equilibrium shifts towards six-coordination in the order, Dy(III) < Ho(III) < Er(III) < Tm(III) < Yb(III), the order of decreasing ionic size. The enthalpies show similar variation to the entropies.

## 4. Coordination structure of bromo complexes

$^{89}$Y-NMR has been measured for the Y(III)–$Br^-$ solution containing ca. 0.1 mol dm$^{-3}$ yttrium(III) and bromide ions in DMF–DMA mixtures. A sharp and single signal indicates that both solvent and ligand exchange rates are fast and signals of all individual species are thus averaged. In Fig. 6, the chemical shift of yttrium(III) bromide solutions relative to the yttrium(III) perchlorate solution $\delta_{Br} - \delta_{ClO_4}$ is plotted against the mole fraction of DMA $x$ in the DMF–DMA mixtures. The chemical shift remains unchanged up to $x = 0.4$, indicating the presence of the outer-sphere complex over the range. At $x > 0.4$, the NMR shifts towards a lower magnetic field with increasing DMA content, indicating that formation of the inner-sphere complex is gradually enhanced.

EXAFS measurements were carried out for a series of DMF–DMA mixtures containing ca. 0.2 mol dm$^{-3}$ $NdBr_3$. Structure function or Fourier transforms $F(r)$ of extracted EXAFS oscillation for Nd(III) is shown in

Fig. 7. The peak at 200 pm is ascribed to the Nd–O (solvent) interaction. The structure function of a $NdBr_3$ DMF solution is the same as that of an $Nd(ClO_4)_3$ DMF solution, indicating that the bromide ion is not coordinated to the metal ion. Note that the structure function of an $Nd(ClO_4)_3$ DMA solution is also the same as that of an $Nd(ClO_4)_3$ DMA solution, as the metal ion is mainly eight-coordinate in both solvents. On the other hand, the structure function of an $NdBr_3$ DMA solution is remarkably different from that of an $Nd(ClO_4)_3$ DMA solution, and the Nd–O (solvent) interaction is significantly weakened in the $NdBr_3$ DMA solution. Besides, as the DMA content increases, a new peak at 250 pm, which is ascribed to the Nd–Br

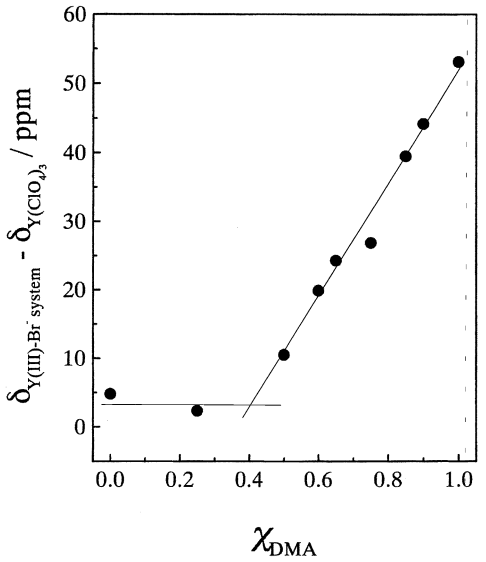


Fig. 6. $^{89}Y$-NMR chemical shift of $YBr_3$ relative to that of $Y(ClO_4)_3$ in the DMF–DMA mixtures, plotted against the mole fraction $x$ of DMA.

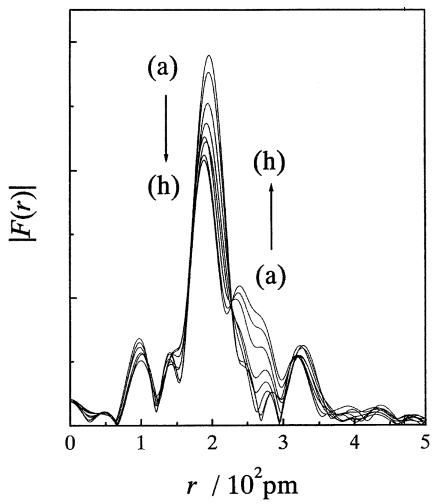


Fig. 7. Fourier transforms $F(r)$ of extracted EXAFS oscillation for $NdBr_3$ in the DMF–DMA mixtures. $x_{DMA} = 0$ (a), 0.25 (b), 0.5 (c), 0.6 (d), 0.65 (e), 0.75 (f), 0.85 (g) and 1 (h).

interaction, becomes more and more intense. On the contrary, the Nd–O (solvent) interaction is weakened with increasing DMA content. As the peak area is proportional to the number of Nd–Br contacts, these clearly provide evidence of the formation of an inner-sphere bromo complex, and the complexation is enhanced with increasing DMA content.

In Fig. 8, Nd–O and Nd–Br bond lengths are plotted against the DMA content $x$, together with the Nd–O bond length obtained in $Nd(ClO_4)_3$ solutions. The Nd–Br interaction is not observed in the $x < 0.5$ mixture despite the fact that the Nd(III) ion forms extensively mono- and di-bromo complexes over the whole range of solvent composition, according to calorimetric measurements. This suggests the formation of outer-sphere bromo complexes in the DMF-rich mixture. The Nd–Br interaction is observed in the $x > 0.5$ mixture, implying that the bromide ion penetrates into the primary coordination sphere to form inner-sphere complexes.

EXAFS measurements have also been carried out for $GdBr_3$, $TmBr_3$ and $YbBr_3$ in the DMF–DMA mixtures. The Ln–O and Ln–Br (Ln = Gd, Tm, Yb) bond lengths are depicted also in Fig. 8, for comparison. The Ln–Br (Ln = Gd, Tm, Yb) interaction is not observed in the $x < 0.5$ mixture, but it does at $x > 0.5$, similar to Nd(III). This implies that, unlike the geometry transition from eight- to seven-coordination of the metal solvate ion, the transition from an outer- to inner-sphere bromo complex is practically independent of the metal ion, or ionic size.

In neat DMF, the Ln–O (Ln = Nd, Gd, Tm, Yb) bond length in the bromide solution is practically the same as that in the perchlorate solution in all the metal systems examined. It is thus established that the solvate Ln–O bond length remains practically unchanged, even if the metal ion forms outer-sphere complexes. The Ln–O bond length observed in the bromide solution decreases in parallel with the formation of inner-sphere bromo complexes in the $x > 0.5$ mixture, and the decreasing profile is not significantly different in all the metal systems examined. The shortening of the Ln–O bond suggests that reduction of the coordination number takes place upon formation of an inner-sphere bromo complex. A variation profile of the Ln–O bond length in the bromide system is quite different from that in the perchlorate system for Nd(III). This is expected because the Nd(III) ion of a relatively large ionic size tends to keep eight-coordination up to $x = 0.8$ in the perchlorate system, while the coordination number may be lowered when an inner-sphere bromo complex is formed at $x > 0.5$ in the bromide system. The same applies also to the Gd(III) system. On the other hand, with Tm(III), the variation profile of the Ln–O bond length in the bromide system is similar to that in the perchlorate system. The Tm(III) ion of a relatively

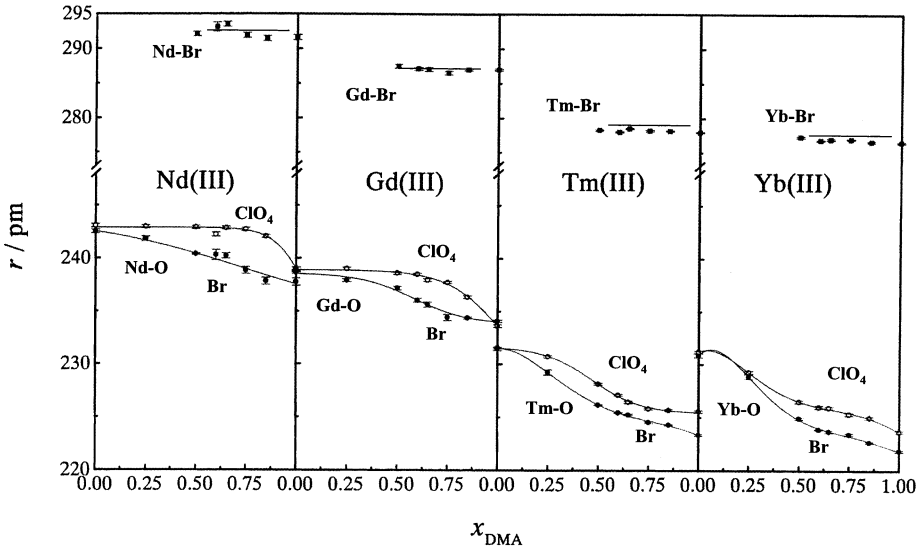


Fig. 8. Variation of the Ln–O (●) and Ln–Br (■) (Ln = Nd, Gd, Tm, Yb) bond lengths in the $LnBr_3$ solution and the Ln–O (○) bond length in the $Ln(ClO_4)_3$ solution plotted against the mole fraction $x$ of DMA. The limit of error bars refers to three standard deviations.

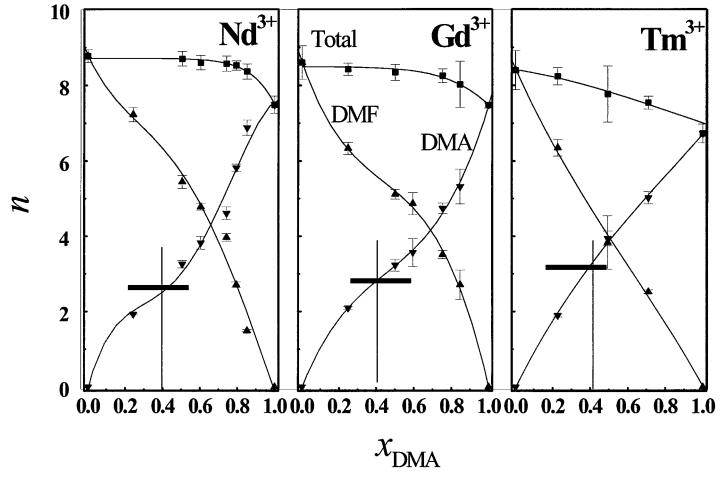


Fig. 9. Total (■) and individual solvation numbers of DMF (▲) and DMA (▼) in the DMF–DMA mixtures plotted against the mole fraction $x$ of DMA.

small ionic size tends to decrease its solvation number from eight to seven almost simultaneously with the formation of inner-sphere bromo complexes.

## 5. Individual solvation number

The outer- to inner-sphere transition for the bromo complex of lanthanide(III) ions occurs in the DMF–DMA mixtures, and the inner-sphere complex starts to form at around 0.4 mol fraction DMA content for all metal ions of varying ionic sizes. On the other hand, the change in the total solvation number from eight to seven in the DMF–DMA mixtures depends strongly on the metal ion. Therefore, the change in the total solvation number is not synchronized with the outer- to inner-sphere transition. It is thus supposed that the individual solvation number of DMA plays a decisive role in the outer- to inner-sphere transition.

Titration Raman spectroscopy allows the determination of individual solvation numbers of DMF and DMA simultaneously coordinating to the metal ion. The detailed procedure of these measurements and analyses is shown elsewhere [12]. The total and individual solvation numbers of DMF and DMA in their mixtures are shown for Nd(III), Gd(III) and Tm(III) in Fig. 9. As seen, the total solvation number, the sum of individual solvation numbers of DMF and DMA, in the DMF–DMA mixtures, shows the same variation profile as that for the Ln–O (solvent) bond length (Fig. 8), clearly indicating that the reduced solvation number leads to a shortening of the metal–solvent bond length.

With increasing DMA content in the DMF–DMA mixtures, the individual DMF solvation number monotonically decreases and the DMA solvation number increases. The variation profile depends on the metal ion. Although, the individual solvation number of DMF in the 0.4 mol fraction DMA content is around 6, 5 and 4 for Nd(III), Gd(III) and Tm(III), respectively, the individual solvation number for DMA is all around 3. This clearly indicates that, when three DMA molecules bind to the metal ion in the DMF–DMA mixtures, the solvation steric effect become significant to lead to the outer- to inner-sphere transition for the bromo complex.

## 6. Conclusions

The solvation steric effect plays an important role in the complexation of metal ions in an aprotic donor solvent. Its dependence on the ionic size of the central metal ion has been studied for a series of lanthanide(III) ions. The solvation number is mainly eight for a series of lanthanide(III) ions in DMF, while it is mainly eight for light Ln(III) but is seven for heavy Ln(III) in DMA, and an equilibrium between seven- and eight-coordination is established for medium Ln(III). Therefore, the geometry change from eight- to seven-coordination takes place in a DMF–DMA mixtures. The mole fraction of DMA at which the geometry change occur depends strongly on the metal ion, and the smaller the metal ion, the lower the DMA content. This is established by means of $^{89}$Y-NMR, EXAFS and Raman spectroscopy.

The thermodynamics of halogeno complexation for a series of lanthanide(III) ions has been studied by titration calorimetry in DMF, DMA and their mixtures. The metal ion forms an outer-sphere complex in DMF, and an inner-sphere complex in DMA, and the transition from outer- to inner-sphere takes place in the mixture. The transition starts to occur in the mixture of 0.4 mol fraction DMA, independent of the metal ion. Consequently, the transition from outer- to inner-sphere bromo complex is controlled by the individual solvation number of DMA. It is found by titration Raman spectroscopy that the outer- to inner-sphere transition starts to occur when three DMA molecules are simultaneously bound to the metal(III) ion.

## References

[1] (a) S. Ishiguro, Bull. Chem. Soc. Jpn. 70 (1997) 1465;
(b) K. Ozutsumi, M. Koide, H. Suzuki, S. Ishiguro, Phys. Chem. 97 (1993) 500;
(c) Y. Inada, K. Sugimoto, K. Ozutsumi, S. Funahashi, Inorg. Chem. 33 (1994) 1875;
(d) S. Ishiguro, K. Ozutsumi, H. Ohtaki, Bull. Chem. Soc. Jpn. 60 (1987) 531;
(e) H. Suzuki, S. Ishiguro, Inorg. Chem. 31 (1992) 4178;
(f) H. Suzuki, M. Koide, S. Ishiguro, J. Chem. Soc. Faraday Trans. 89 (1993) 3055;
(g) M. Koide, S. Ishiguro, J. Chem. Soc. Faraday Trans. 91 (1995) 2313;
(h) M. Koide, H. Suzuki, S. Ishiguro, J. Chem. Soc. Faraday Trans. 91 (1995) 3851;
(i) H. Suzuki, M. Koide, S. Ishiguro, Bull. Chem. Soc. Jpn. 67 (1994) 1320;
(j) H. Suzuki, S. Ishiguro, Acta Crystallogr. Sect. c 53 (1997) 1602;
(k) S. Ishiguro, Y. Umebayashi, M. Komiya, Y. Nagahama, Y. Kobayashi, J. Chem. Soc. Faraday Trans. 94 (1998) 647;
(l) S. Ishiguro, K. Ozutsumi, H. Ohtaki, J. Chem. Soc. Faraday Trans. 1 84 (1988) 2409;
(m) Y. Abe, K. Ozutsumi, S. Ishiguro, J. Chem. Soc. Faraday Trans. 1 85 (1989) 3747;
(n) Y. Abe, S. Ishiguro, J. Solution Chem. 20 (1991) 793;
(o) Y. Abe, K. Ozutsumi, R. Takahashi, S. Ishiguro, J. Chem. Soc. Faraday Trans. 88 (1992) 1997;
(p) K. Ozutsumi, Y. Abe, R. Takahashi, S. Ishiguro, J. Phys. Chem. 98 (1994) 9894.

[2] (a) S.P. Sinha, Nato ASI Ser. C 109 (1983) 71 and 451;
(b) P.M. Grant, P. Robouch, R.A. Torres, P.A. Baisden, R.J. Silva, J. Solution Chem. 21 (1992) 213;
(c) J.H. Forsberg, T.J. Dolter, A.M. Carter, D. Singh, S.A. Aubuchon, A.T. Timperman, A. Ziaee, Inorg. Chem. 31 (1992) 5555;
(d) Z. Chen, C. Deterier, Can. J. Chem. 72 (1994) 1753;
(e) W. D'Olieslager, A. Oeyen, Radiochim. Acta 61 (1993) 213;
(f) P.S. Coan, L.G. Hubert-Pfalzgraf, K.G. Caulton, Inorg. Chem. 31 (1992) 1261;
(g) A. Fratieo, V. Kubo-Anderson, E. Bolanos, O. Chaves, F. Laghaei, J.V. Ortega, R.D. Perrigan, F. Reyes, J. Solution Chem. 23 (1994) 1019;
(h) G. Adachi (Ed.), New development of studies on rare earth complexes, Report of a priority area research program 1994–1997, Daitoinsatsu, Osaka, 1997.

[3] (a) R.J. Mumper, M. Jay, J. Phys. Chem. 96 (1992) 8626;
(b) F. Arnaud-Neu, Chem. Soc. Rev. 23 (1994) 235;
(c) C. Piguet, J.-C. Bünzli, Chem. Soc. Rev. 28 (1999) 347.

[4] (a) S. Ishiguro, K. Kato, R. Takahashi, S. Nakasone, Rare Earths 27 (1995) 61;
(b) S. Ishiguro, R. Takahashi, Inorg. Chem. 30 (1991) 1854;
(c) R. Takahashi, S. Ishiguro, J. Chem. Soc. Faraday Trans. 88 (1992) 3165.

[5] (a) P.D. Bernardo, G.R. Choppin, R. Portanova, P.L. Zanonato, Inorg. Chim. Acta 207 (1993) 85;
(b) A. Cassol, G.R. Choppin, P.D. Bernardo, R. Portanova, M. Tolazzi, G. Tomat, P.L. Zanonato, J. Chem. Soc. Dalton Trans. (1993) 1695;
(c) M. Frechette, I.R. Butler, R. Hynes, C. Detellier, Inorg. Chem. 31 (1992) 1650;
(d) Z. Chen, C. Detellier, Can. J. Chem. 72 (1994) 1797;
(e) A. Milicic-Tang, J.G. Bünzli, Inorg. Chim. Acta 192 (1992) 201;
(f) Z. Wang, G.R. Choppin, P.D. Bernardo, P.L. Zanonato, R. Portanova, M. Tolazzi, J. Chem. Soc. Dalton Trans. (1993) 2791;
(g) A. Cassol, P.D. Bernardo, R. Portanova, M. Tolazzi, G. Tomat, P.L. Zanonato, J. Chem. Soc. Dalton Trans. 1 (1992) 469;
(h) J.-C. Bünzli, Handbook on the Physics and Chemistry of Rare Earths, vol. 21, Elsevier, Amsterdam, 1995, p. 306.

[6] (a) J. Legendziewicz, K. Bukietynska, G. Oczko, S. Ernst, B. Jezowska-Trzebiatowska, Chem. Phys. Lett. 73 (1980) 576;
(b) J. Legendziewicz, K. Bukietynska, G. Oczko, J. Inorg. Nucl. Chem. 43 (1981) 2391;
(c) J. Legendziewicz, B. Keller, W. Strek, Chem. Phys. Lett. 92 (1982) 205;
(d) J. Legendziewicz, Bull. Acad. Polish Sci. 33 (1985) 147;
(e) J. Legendziewicz, Bull. Acad. Polish Sci. 33 (1985) 305;
(f) J. Legendziewicz, G. Oczko, B. Keller, Bull. Acad. Polish Sci. 34 (1986) 257;
(g) G. Oczko, J. Legendziewicz, B. Keller, B. Jezowska-Trzebiatowska, Spectrochim. Acta 9 (1989) 945.
[7] R. Takahashi, S. Ishiguro, J. Chem. Soc. Faraday Trans. 87 (1991) 3379.
[8] V. Gutmann, The Donor–Acceptor Approach to Molecular Interactions, Plenum Press, New York, 1978.
[9] S. Ishiguro, K. Kato, S. Nakasone, R. Takahashi, K. Ozutsumi, J. Chem. Soc. Faraday Trans. 92 (1996) 1869.
[10] S. Ishiguro, Y. Umebayashi, K. Kato, R. Takahashi, K. Ozutsumi, J. Chem. Soc. Faraday Trans. 94 (1998) 3607.
[11] S. Ishiguro, Y. Umebayashi, K. Kato, S. Nakasone, R. Takahashi, Chem. Phys. Phys. Chem. 1 (1999) 2775.
[12] Y. Umebayashi, K. Matsumoto, M. Watanabe, K. Katoh, S. Ishiguro, Anal. Sci. 17 (2001) 323.
[13] A. Haubenschuss, F.H. Spedding, J. Chem. Phys. 70 (1979) 2797.
[14] A. Haubenschuss, F.H. Spedding, J. Chem. Phys. 70 (1979) 3758.
[15] A. Haubenschuss, F.H. Spedding, J. Chem. Phys. 73 (1980) 442.
[16] T. Yamaguchi, M. Nomura, H. Wakita, H. Ohtaki, J. Chem. Phys. 89 (1988) 5133.
[17] C. Cossy, A.E. Merbach, Pure Appl. Chem. 60 (1988) 1785.
[18] L. Helm, A.E. Merbach, Eur. J. Solid State Inorg. Chem. 28 (1991) 245.
[19] T. Moeller, R. Ferrus, J. Inorg. Nucl. Chem. 20 (1961) 261.